Electroclinic effect in the chiral lamellar α phase of a lyotropic liquid crystal

Marc D. Harjung and Frank Giesselmann*
Institute of Physical Chemistry, University of Stuttgart, Pfaffenwaldring 55, 70569 Stuttgart, Germany

(Received 22 December 2017; published 30 March 2018)

In thermotropic chiral Sm-A^* phases, an electric field along the smectic layers breaks the D_∞ symmetry of the Sm-A^* phase and induces a tilt of the liquid crystal director. This so-called electroclinic effect (ECE) was first reported by Garoff and Meyer in 1977 and attracted substantial scientific and technological interest due to its linear and submicrosecond electro-optic response [S. Garoff and R. B. Meyer, Phys. Rev. A **19**, 338 (1979)]. We now report the observation of an ECE in the pretransitional regime from a lyotropic chiral lamellar L_α^* phase into a lyo-Sm-C^* phase, the lyotropic analog to the thermotropic Sm-C^* phase which was recently discovered by Bruckner *et al.* [Angew. Chem. Int. Ed. **52**, 8934 (2013)]. We further show that the observed ECE has all signatures of its thermotropic counterpart, namely (i) the effect is chiral in nature and vanishes in the racemic L_α phase, (ii) the effect is essentially linear in the sign and magnitude of the electric field, and (iii) the magnitude of the effect diverges hyperbolically as the temperature approaches the critical temperature of the second order tilting transition. Specific deviations between the ECEs in chiral lamellar and chiral smectic phases are related to the internal field screening effect of electric double layers formed by inevitable ionic impurities in lyotropic phases.

DOI: 10.1103/PhysRevE.97.032705

I. INTRODUCTION

In 1977, Garoff and Meyer reported the observation of the electroclinic effect (ECE) in thermotropic chiral smectic liquid crystals, namely in a smectic-*A* phase composed of chiral molecules (Sm-A^*) [1,2]. An electric field **E** directed along the Sm-A^* layers induces a collective molecular tilt, the direction of which is normal to both the smectic layer normal **k** and the field **E**. The magnitude of induced tilt $\delta\theta$ between the liquid crystal director **n** and the smectic layer normal **k** basically increases linearly with E. Since the Sm-A^* director represents its optic axis, the ECE thus gives rise to a linear and very fast electro-optic effect, which has received substantial scientific and technological interest [3].

The origin of the ECE was explained by a general symmetry argument: the electric field along the Sm-A^* layers preferentially aligns the transverse permanent dipoles of the rodlike molecules in the direction of E and thereby biases the rotation of the molecules about their long axes [1,2]. Since in a chiral medium the plane containing the induced polarization **P** and **k** is no mirror plane (contrary to the case of a nonchiral smectic-*A*), the free energy of molecular tilt is nonsymmetric about the **k**, **P** plane. As a result, a nonzero director tilt is observed relative to **k**. In other words, according to the Curie principle, the polar vector of the electric field reduces the D_∞ symmetry of the undisturbed Sm-A^* phase to the polar point group C_2, the point group of a chiral ferroelectric smectic-C^* (Sm-C^*) phase [4]. That allows a director tilt normal to the C_2 axis, which is the direction of the field **E**.

This symmetry argument, however, predicts neither the sign nor the magnitude of the induced tilt. In practice, a measurable ECE is only observed in the vicinity of a second-order (or weak first-order) transition into the tilted Sm-C^* phase, typically a few kelvin above the critical phase transition temperature T_c^*. In this pretransitional temperature regime, thermal fluctuations of the tilt angle become large ("soft mode") [5] and in first approximation the electroclinically induced tilt $\delta\theta$ diverges according to a Curie-Weiss-like behavior [6]:

$$\delta\theta = \frac{\varepsilon_0 \chi_0 C}{\alpha(T - T_c^*)} E, \tag{1}$$

where $T > T_c^*$ denotes the temperature, α is the coefficient of the quadratic term in the Landau free energy expansion, ε_0 is the vacuum permittivity, χ_0 is the high-frequency dielectric susceptibility, and C is the bilinear coupling coefficient between polarization and tilt. In certain de Vries–type smectics $\delta\theta$ reaches values up to 15° at $E = 10\ \mathrm{V}/\mu\mathrm{m}$ and $T - T_c^* = +1$ K [7,8]. The ECE is sometimes considered as a kind of liquid crystal analog [9] to the piezoelectric effect in solid crystals since the "deformation" $\delta\theta$ is linear in E. The induced tilt however is an angular variable [10–12] and the fluid Sm-A^* phase does not support static shear stains as in the case of solid piezoelectrics. Similarities and differences between the ECE and piezoelectricity have been comprehensively discussed by Lagerwall *et al.* [3,5,13–15].

The lyotropic analog to the thermotropic Sm-A^* phase is the chiral variant of the well known lamellar α phase [L_α^*; see Fig. 1(a)]. This phase is composed of (nonmesogenic) amphiphilic molecules, which aggregate into fluid bilayers. Adjacent bilayers are separated from each other by fluid layers of small solvent molecules (e.g., water) and the director **n** of the amphiphilic molecules is along the bilayer normal **k**, schematically drawn in Fig. 1(a). As the bilayers are composed of chiral amphiphiles, the lamellar phase lacks any mirror symmetry and has D_∞ symmetry. As a result of its chirality, the symmetry argument discussed above applies in the very

*f.giesselmann@ipc.uni-stuttgart.de

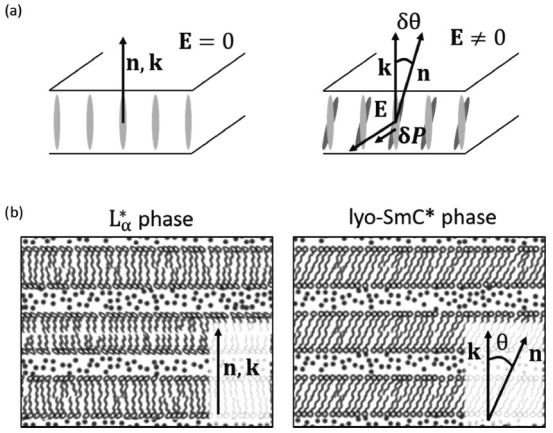

FIG. 1. (a) Schematic representation of the ECE in chiral Sm-A^* phases. At zero electric field, the director **n** is parallel to the smectic layer normal **k** (left). Application of an electric field E in a direction along the smectic layer planes induces a polarization δP normal to **n** and **k** and gives rise to an induced tilt angle $\delta\theta$ due to the coupling between polarization and tilt in chiral smectics. (b) Structure of the well-known lyotropic lamellar α^* phase with its director **n** parallel to **k** (left). The L^*_α phase is the lyotropic analog to the thermotropic smectic A^* phase. Successive bilayers of surfactant molecules are separated from each other by layers of solvent molecules (•). Structure of the lyo-Sm-C^* phase (right). The surfactant molecules are uniformly tilted within each bilayer. Since the direction of tilt is the same in all bilayers (synclinic correlation), the global director **n** is tilted with respect to the layer normal **k**.

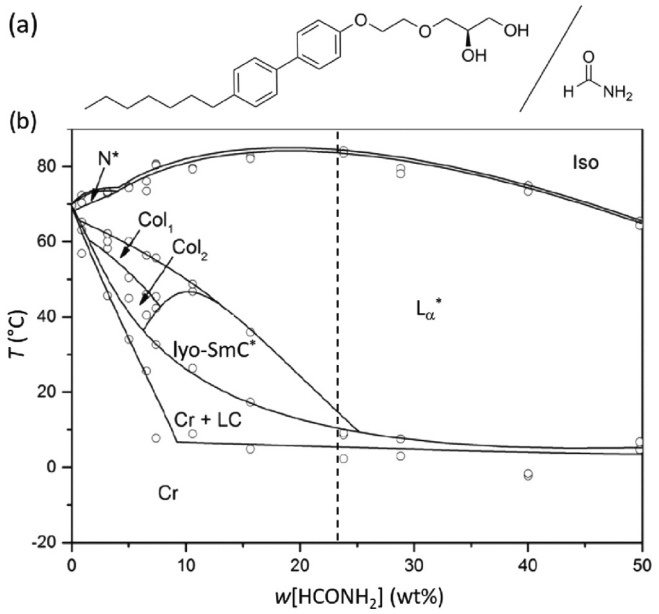

FIG. 2. (a) Molecular structure of the chiral amphiphile **G10** and the solvent formamide. (b) Phase diagram of the binary system **G10**/formamide. Between 15 and 25 wt. % of formamide a lyotropic analog of the Sm-A^*–Sm-C^* transition in thermotropic liquid crystal is found. The dashed line indicates the composition of the sample investigated in this study [18].

same way to L^*_α as in the case of Sm-A^* and thus an ECE should also be expected for the lyotropic L^*_α phase.

A first indication of an ECE in lamellar phases is the observation of piezoelectricity in the Sm-A^* phase of chiral phospholipid bilayers [16,17]. But, to the best of our knowledge, there is no clear-cut report on the observation of an ECE in chiral lyotropic L^*_α phases so far. One reason for this is certainly the high electrode polarization of lyotropic phases that complicates the application of static or low-frequency electric fields. Another important reason is that the lyotropic analog to the thermotropic Sm-C^* phase was unknown until the report of Bruckner *et al.* in 2013 [18,19]. Here, the chiral amphiphilic compound **G10** was shown to form a first example of a chiral, fluid, and tilted lamellar phase [named lyo-Sm-C^* or $L^*_{\alpha'}$; see Fig. 1(b)] with water or formamide as solvents. At higher temperatures, the lyo-Sm-C^* phase transforms into a nontilted L^*_α phase [see phase diagram in Fig. 2(b)]. The presence of a tilting transition from a nontilted L^*_α phase into a tilted lyo-Sm-C^* phase with long-range correlated synclinic tilt directions was confirmed in earlier 2D-XRD [18] and micro-Raman experiments [19]. This opens the unique opportunity to study this tilting transition in the case of lyotropic lamellar phases.

As a result of these studies we now report that a substantial ECE is indeed observed in the pretransitional regime from the nontilted L^*_α into the tilted lyo-Sm-C^* phase. The properties of this lyotropic ECE are widely analog to its thermotropic counterpart. In particular, the induced tilt $\delta\theta$ is linear in E and diverges on approaching T^*_c. Since a biological phospholipid membrane can be considered as a single L^*_α bilayer with chiral inclusions (such as cholesterol or transmembrane proteins), these results might also have implications for the physics of biomembranes [20–23].

II. EXPERIMENT

Samples of the lyotropic lamellar phase are prepared from the chiral amphiphile **G10** [Fig. 2(a)] with highly purified formamide and filled into liquid crystal test cells with 1.6 μm cell gap, transparent ITO electrodes, and rubbed nylon coatings. Since nylon coatings are known to produce planar alignment in many thermotropic smectics [24–26], we tried nylon coatings as well to study our lyotropic system and indeed obtained planar alignment in the so-called bookshelf configuration of the lamellar layers in L^*_α. During the tilting transition into the lyo-Sm-C^* phase the formation of chevron layer configurations with zig-zag defects was observed [27–31]. The cell is placed in the hot stage of a polarizing optical microscope, connected to an electric ac waveform generator and the intensity of light transmitted through the cell between crossed polarizers detected by a photodiode. Precise temperature control was achieved by electrical heating against liquid N_2 cooling. Further experimental details are found in Appendix A. To obtain maximum amplitude of electro-optic response the cell is fixed such that its optical axis (i.e., its director) at zero electric field includes an azimuth angle of $\varphi_0 = \pi/8$ (22.5°) with the polarizer direction [see also Fig. 3(b)] [3]. If the director deviates from its zero-field orientation φ_0 by an electroclinically induced tilt $\delta\theta$, the intensity of transmitted

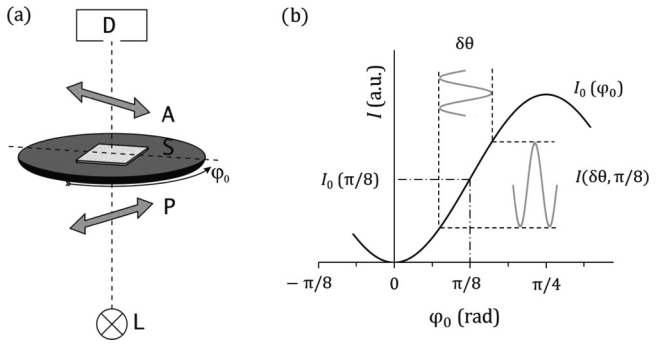

FIG. 3. (a) Schematic beam path in the setup for electro-optic measurements. I: light source; P: polarizer; A: analyzer (crossed to P); D: detector; φ_0: angle between polarization plane of incoming light and optical axis (director) of the sample S at zero electric field. (b) At $\varphi_0 = \pi/8$ (22.5°) the intensity response $I(\delta\theta)$ to a small (electroclinic) variation of the director tilt ($\delta\theta$) is maximized and linear.

light I of the sample between crossed polarizers varies as

$$I = \sin^2(2(\varphi_0 + \delta\theta))\sin^2\left(\frac{\Delta_0}{2}\right), \tag{2}$$

where φ_0 denotes the optical retardation of the sample which remains unchanged by the electric field since the electroclinic tilt is induced normal to the light path and thus does not change the birefringence of the sample. Taylor series expansion of $\sin^2(2(\varphi_0 + \delta\theta))$ at $\varphi_0 = \pi/8$ leads to

$$I(\delta\theta) = \left(\frac{1}{2} + \sqrt{2}\delta\theta + \cdots\right)\sin^2\left(\frac{\Delta_0}{2}\right) \tag{3}$$

and shows that I varies linearly with a small electroclinic tilt $\delta\theta$. With $I_0 = \sin^2(\Delta_0/2)/2$ being the transmitted light intensity at zero electric field ($\delta\theta = 0$), the electroclinic tilt is finally obtained as

$$\delta\theta = \frac{1}{\sqrt{2}}\left(\frac{I(\delta\theta)}{I_0} - 1\right) \tag{4}$$

from field-dependent measurements of the transmitted light intensity $I(\delta\theta)$. In the following section we will discuss the characteristics of the ECE in a lyotropic example and want to show that the behavior is widely analog to the pretransitional chirality effect of thermotropic Sm-A^* phases.

III. RESULTS AND DISCUSSION

The following experiments were carried out with a lyotropic sample containing 23.5 wt. % of the chiral amphiphile **G10** in formamide. After filling the material into the nylon-coated glass cells, the chiral L_α^* phase shows rather uniform planar alignment [Fig. 4(a)]. At temperatures below $T_c^* = 13.5\,^\circ$C the formation of well-defined tilt domains is seen Fig. 4(b), the presence of which indicates the phase transition into the tilted lyo-Sm-C^* phase with a continuously growing tilt at further decreasing temperature. Previous investigations also revealed that the tilting transition is second order for this composition of the lamellar phase [19]. In the L_α^* phase and at temperatures T slightly above T_c^*, the application of an ac electric field along the lamellar layers induces a distinct

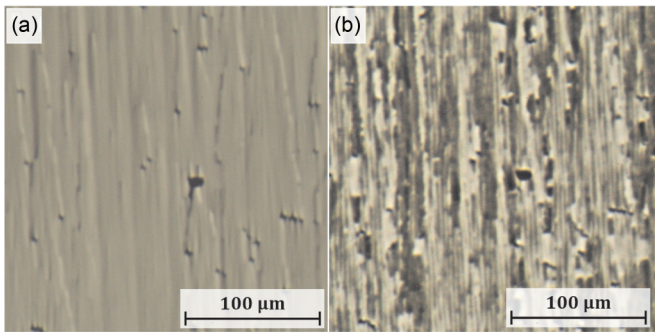

FIG. 4. (a) POM image of the planar aligned chiral lamellar L_α^* phase in a bookshelf configuration at 15 °C. (b) Tilt domains and zig-zag defects in the planar aligned lyo-Sm-C^* phase at 10 °C ($T_c^* = 13.5\,^\circ$C). For lyotropics, the birefringence in the order of $\delta n \approx 0.1$ is rather high due to the presence of highly polarizable aromatic cores [32].

electro-optic modulation. An example is seen in Fig. 5 where the application of an ac electric square wave field [Fig. 5(a)] with 400 Hz frequency and 1.9 V/μm amplitude leads at $T - T_c^* = +0.2$ K to a distorted square wave response in the transmission of the chiral L_α^* sample between crossed polarizers [black curve in Fig. 5(b)]. In a control experiment we replaced the chiral **G10** by racemic **G10** and the result was that under the same conditions as before no electro-optic response could be detected from the now nonchiral L_α phase [red curve in Fig. 5(b)]. This clear connection between the presence of chirality and the observation of an electro-optic response of the material strongly suggests an ECE as the origin of the electro-optic response of the chiral L_α^* phase.

We further investigated the electro-optic response of the L_α^* phase to three different waveforms of the ac electric field applied. Selected results are presented in Fig. 6, where all transmitted intensity data $I(t)$ were converted into time-dependent director tilt angles $\delta\theta(t)$ (see Sec. II) and compared to the respective electroclinic response of a typical thermotropic Sm-A^* phase, namely the Sm-A^* phase of the FLC mixture Felix 4851/050 from Clariant. The experimental results in Fig. 6 lead us to the following observations.

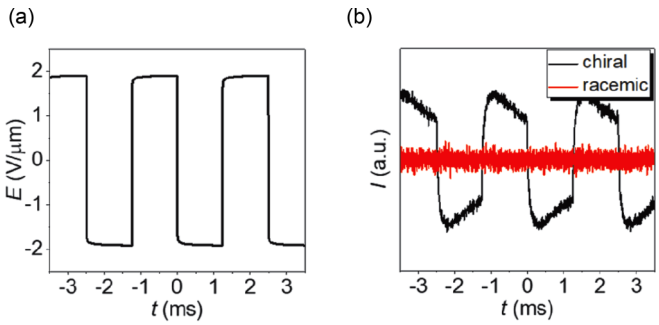

FIG. 5. (a) Square-wave electric field $E(t)$ applied to the lyotropic sample in a direction normal to the director **n**. (b) Response in the transmitted light intensity I of the lyotropic sample to the $E(t)$ in (a) 0.2 K above the transition temperature into the tilted phase; black line: chiral L_α^* phase with 23 wt. % formamide; red line: racemic L_α phase with same composition.

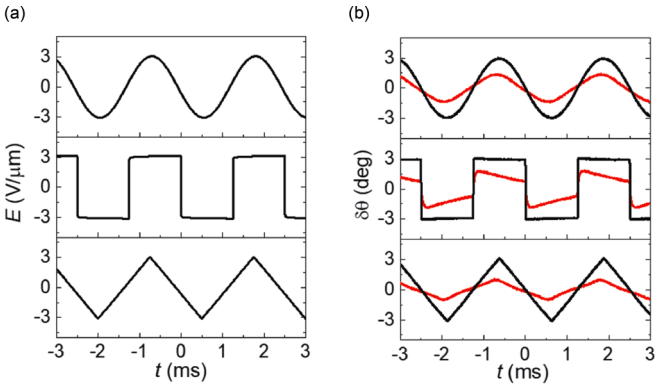

FIG. 6. (a) Various waveforms of the ac electric field, applied normal to the director **n**. (b) Comparison of the electroclinic response to the corresponding waveforms in case of the lyotropic lamellar α^* phase with 23 wt. % formamide (red line) and in the case of the thermotropic Sm-A^* phase of Felix 4851/050 (black line).

(i) The amplitude of the lyotropic L_α^* response is slightly smaller than but in the same order of magnitude as the electroclinic response of the thermotropic Sm-A^* phase.

(ii) At first glance, the lyotropic L_α^* response is essentially linear to the sign and the strength of the applied electric field E, at least in the sense that a quadratic response (which would be doubled in frequency) can be excluded.

(iii) The lyotropic L_α^* response however certainly deviates from a strict linear response. These deviations are most obvious in the case of a square wave electric field: in contrast to the thermotropic Sm-A^* response, the L_α^* response slightly relaxes in time while the field strength remains constant.

The latter observation deserves a closer consideration since it describes a significant deviation from pure electroclinic behavior. From an experimentalist point of view, a major difference between thermotropic and lyotropic liquid crystal materials is the high electric conductivity of lyotropics due to the presence of ionic impurities in the solvent. Ionic migration in an electric field leads to the formation of electric double layers at the interfaces between the solid electrodes and the liquid-crystalline electrolyte. These double layers screen the external electric field and thus reduce the effective field inside the liquid crystal layer.

This screening effect is clearly seen in Fig. 7, where the ECE response of the thermotropic Felix 4851/050 is compared to the ECE of the lyotropic **G10** with 23 wt. % formamide in the frequency domain. The ECE follows a Cole-Cole relaxation [33]:

$$\delta\theta^*(\omega) = \frac{\delta\theta_{\max}}{1 + (i\omega\tau)^{a_{cc}}}, \tag{5}$$

with relaxation strengths $\delta\theta_{\max}$, relaxation time τ, and distribution parameter a_{cc} (fitting parameter, see Table I). The slowing down of the relaxation time τ, typical of the electroclinic soft-mode effect close to T_c^*, is observed in both thermotropic Sm-A^* and lyotropic L_α^* (see Table I).

In the lyotropic case, however, negative deviation from the Cole-Cole relaxation is observed towards lower frequencies. These deviations are attributed to the ionic screening effects,

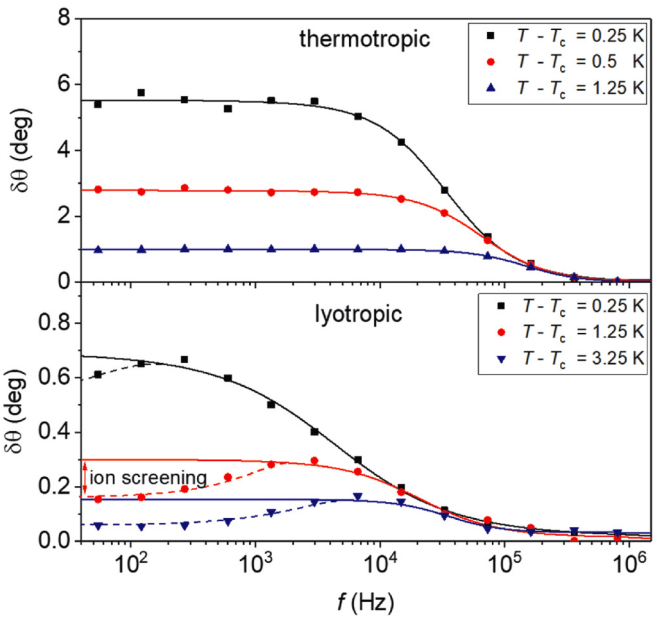

FIG. 7. Frequency-dependent measurements of the ECE within the thermotropic Sm-A^* phase of Felix 4851/050 as well as in the lyotropic L_α^* phase of **G10** with 23 wt. % formamide by applying an external field of various frequencies and 2 V/μm amplitude. In case of the thermotropic phase, the ECE shows a Cole-Cole relaxation behavior, while the ECE of the lyotropic L_α^* phase is reduced at lower frequencies.

which are found to be about one order of magnitude slower than the ECE itself.

The screening effect and its impact on electro-optic effects is well known in thermotropic liquid crystals such as thermotropic nematics [34–38] and thermotropic Sm-C^* phases [39–44]. In highly purified thermotropic materials, such as the Felix 4851/050 material used for the measurements in Figs. 6 and 7, the screening effect is negligibly small. In our case of a lyotropic L_α^* material, however, ion concentration and electric conductivity are much higher due to the presence of polar and protic solvents such as water or formamide. Even though our formamide solvent was intensively purified, residual amounts of ionic impurities are inevitable, i.e., due to the hydrolysis of formamide with moisture [45–47]. As a result of their substantial electrolytic conductivity, the application of an electric dc field in the order of a view V/μm leads

TABLE I. Fitting parameters of the frequency-dependent ECE response described by a Cole-Cole relaxation process in the case of the thermotropic Sm-A^* phase of Felix 4851/050 as well as of the lyotropic L_α^* phase of **G10** with 23 wt. % formamide.

	$T - T_c^*$ (K)	$\delta\theta_{\max}$ (deg)	τ (μs)	a_{cc}
Thermotropic	0.25	5.5	4.71	0.88
	0.5	2.8	2.42	0.92
	1.25	1.0	1.08	0.99
Lyotropic	0.25	0.7	36.6	0.67
	1.25	0.3	7.69	0.84
	3.25	0.1	4.58	1.00

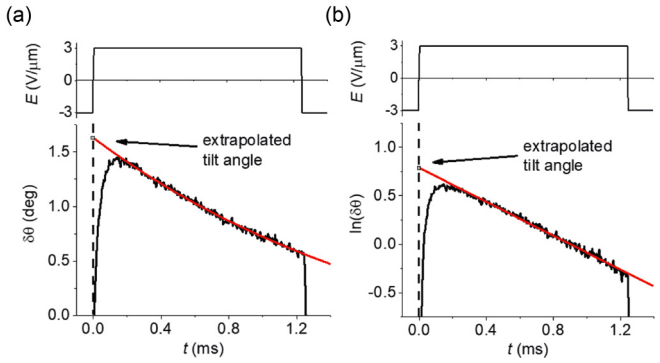

FIG. 8. (a) Induced tilt angle response $\delta\theta(t)$ of the L_α^* phase to a square-wave electric field $E(t)$. The slow relaxation of $\delta\theta(t)$ during a single half-cycle of $E(t)$ is well described by a monoexponential decay. (b) Semilogarithmic plot of the $\delta\theta(t)$ data shown in (a). The linear extrapolation of $\delta\theta(t)$ to the time of field reversal leads to a corrected tilt angle which is less affected by ion screening effects.

to (electrolytic) degradation of the L_α^* samples after a few minutes. We thus propose that the observed deviations from a pure electroclinic response originate from the screening effects of the ionic impurities. The relevance of ionic screening effects was further supported by experiments in which we deliberately increased the ionic concentration in the L_α^* phase and observed a decreasing amplitude of the electroclinic response (see Appendix B).

Since the electroclinic response probes the effective field inside the L_α^* layer between the electrodes, its decay in time reflects the dynamics of electric double layer formation. As seen in Fig. 8, the slow relaxation of the electronic tilt $\delta\theta(t)$ during a half-cycle of a square-wave electric field follows a monoexponential rate law. The extrapolation of $\delta\theta(t)$ to the time of field reversal (Fig. 8) enables a simple correction to obtain the "true" electroclinic tilt $\delta\theta(t)$, which would be expected in the absence of any ionic screening effects.

Based on such corrected $\delta\theta$ data we now examine how the field-induced director tilt of the L_α^* phase varies with temperature and electric field strength. At a fixed temperature of 0.5 K above the tilting transition we applied a 400 Hz square-wave electric field, the amplitude of which was continuously increased from 0.3 to 3.1 V/μm (higher field amplitudes led to a decomposition of the sample at around 3.5 V/μm). As seen in Fig. 9(a), the electroclinic response of the L_α^* sample increases as the field amplitude increases. The corrected values of the induced tilt are plotted vs the electric field amplitude in Fig. 9(b). Above a certain threshold field of about 1.5 V/μm the induced tilt angle $\delta\theta$ increases linear with the field strength E. While the linearity of $\delta\theta(E)$ is a clear signature of the electroclinic effect, the presence of a threshold field is not.

We assume that this deviation from pure electroclinic behavior originates again from ionic impurities and the dynamics of electric double layer formation. The charge reversal of the electric double layers—starting at the time of external field reversal—is a nontrivial electrochemical process, the dynamics and the effect of which are certainly not fully corrected by the simple extrapolation procedure described above and might thus lead to the apparent threshold behavior seen in Fig. 9(b). Finally, we investigated the temperature dependence of the

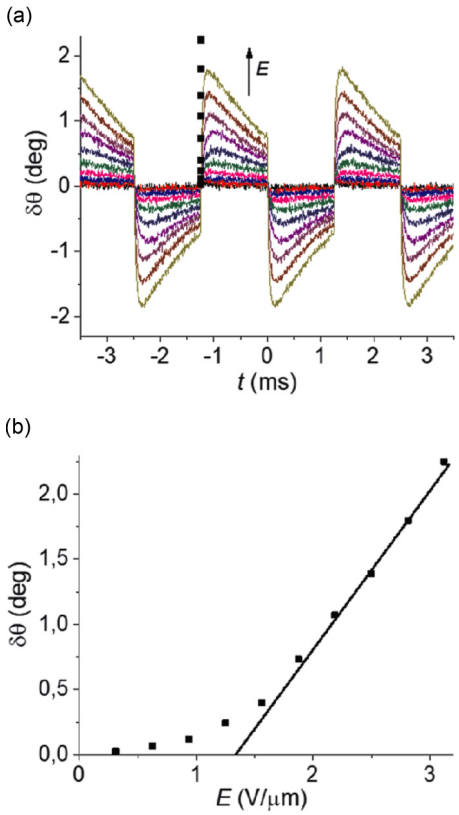

FIG. 9. (a) Electroclinic response $\delta\theta(t)$ of the L_α^* phase to a square-wave electric field with 400 Hz frequency and amplitude E increasing from 0.3 to 3.1 V/μm at a fixed temperature of $T - T_c^* = 0.5$ K. (b) Plot of corrected values of the induced tilt $\delta\theta$ vs electric field strength E. The straight line shows the linear regime of $\delta\theta(E)$.

induced tilt angle in the L_α^* phase. We applied a square-wave electric field with a fixed amplitude of 1.9 V/μm, well above the (apparent) threshold field, and measured the induced tilt angle response of the L_α^* phase, while slowly cooling from 20 °C to the tilting transition temperature at $T_c^* = 13.5$ °C. The tilt angle response $\delta\theta(t)$ drastically increases with decreasing temperature [Fig. 10(a)] and corrected values of the induced tilt hyperbolically diverge as T approaches T_c^* [Fig. 10(b)]. This result is in perfect agreement with the electroclinic effect in thermotropic materials approaching a second order Sm-A^*–Sm-C^* transition and, in particular, with Eq. (1) describing the Curie-Weiss-like behavior of the electroclinic effect. The slope in the linear regime of $\delta\theta(E)$ in Fig. 9(b) indicates an electroclinic coefficient $e_c = (\partial\theta/\partial E)$ of the lyotropic L_α^* phase in the order of 10^{-6} deg m V^{-1} at $T - T_c^* = 0.5$ K, a value which is actually in the same order of magnitude as electroclinic coefficients of thermotropic Sm-A^* phases [48–55]. According to Eq. (1), the electroclinic coefficient at a given value of $T - T_c^*$ is determined by the ratio of the coupling term $\varepsilon_0\chi_0 C$ and the leading coefficient α in the Landau free energy expansion. However, any thorough analysis of these terms requires accurate measurements of P_s, which are—due to the high conductivity of lyotropics—not available so far. Instead we compare the ratios $\kappa = \varepsilon_0\chi_0 C/\alpha = e_c(T - T_c^*)$ of these terms. With $\kappa_{lyo} = 5 \times 10^{-9}$ m V^{-1} K, this ratio is comparable to those of typical thermotropic materials, such

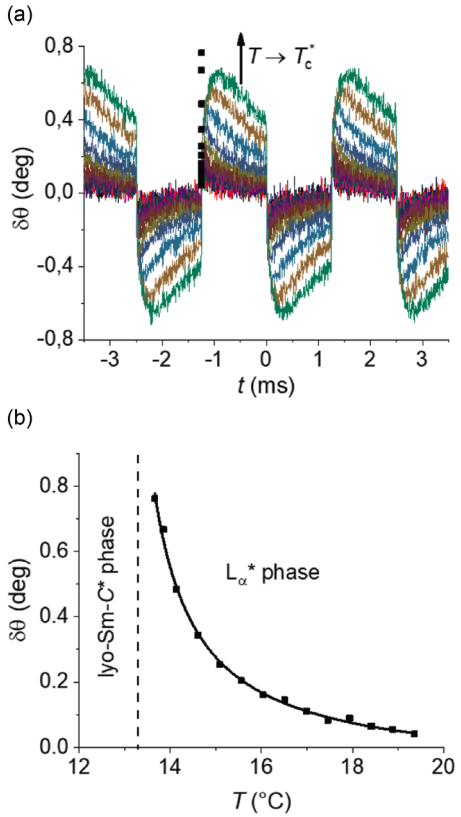

FIG. 10. (a) Electroclinic response $\delta\theta(t)$ of the L_α^* phase to a square-wave electric field with 400 Hz frequency and an amplitude of 1.9 V/μm at decreasing temperatures approaching the transition temperature T_c^* into the lyo-Sm-C^* phase. (b) Plot of corrected values of the induced tilt $\delta\theta$ vs temperature T. The solid line shows the hyperbolic divergence of $\delta\theta(T - T_c^*)$.

as DOBAMBC [(2–3) $\times 10^{-9}$ m V^{-1} K [48,49]], FLC 10288 (9×10^{-9} m V^{-1} K [50]), or FLC 6430 (24×10^{-9} m V^{-1} K [50]). Since the spontaneous electric polarization of the lyo-Sm-C^* phase and thus the coupling term $\varepsilon_0\chi_0 C$ are assumed to be at least one order of magnitude smaller than in thermotropic chiral smectics [56,57], the experimental observation of comparable ratios κ in thermotropics and lyotropics requires that the Landau coefficient α of lyotropic L_α^* is at least one order of magnitude smaller than in thermotropic smectics. A lower value of α implies that changes in θ require less energy and—since changes in θ also change the layer thickness—that the bilayers in lyotropic L_α^* are more compressible than the smectic layers in thermotropic Sm-A^*. This is in good agreement with the very low elastic moduli found in the L_α phases of lipid bilayers [58–62].

IV. CONCLUSION

In the pretransitional regime from a chiral lyotropic L_α^* phase into the lyo-Sm-C^* phase we observed a clear electro-optic effect which has all signatures of the well-known electroclinic effect in thermotropic Sm-A^*, namely (i) the effect is chiral in nature and vanishes in the racemic L_α phase, (ii) the effect is essentially linear in the sign and magnitude of the electric field, and (iii) the magnitude of the effect diverges hyperbolically as the temperature T approaches the tilting transition temperature T_c^*. We thus conclude that the electroclinic effect exists in chiral lyotropic L_α^* phases and can be experimentally observed as fast electro-optic switching of L_α^* phases in the pretransitional regime of a tilting transition. About 40 years after the discovery of the ECE in thermotropic smectics, this is an experimental proof that the symmetry arguments of Garoff and Meyer apply to chiral lyotropic phases in the very same way as to chiral thermotropic smectics.

Specific deviations between the ECEs in chiral lamellar and chiral smectic phases can at least in a qualitative way be explained by the internal field screening effect of electric double layers formed by ionic impurities. It turned out that the ECE was only observable when solvent was highly purified such that its conductivity was below a few μS/cm the sample conductivity was reduced to a high degree.

Further research will be directed to better understand how the dynamics of electric double layer formation and internal field screening superimposes the ECE in chiral lamellar phases. Another open point is the following question: how far can the molecular picture of the ECE in chiral smectics be applied to chiral lamellar phases? Finally, the existence of an ECE in chiral lamellar phases might have certain implications in the field of biomembrane physics since phospholipid membranes are basically single L_α^* bilayers including chiral molecules such as cholesterol or transmembrane proteins.

ACKNOWLEDGMENT

We thank the Deutsche Forschungsgemeinschaft (DFG Gi Grant No. 243/4) for financial support.

APPENDIX A: EXPERIMENTAL DETAILS

Electro-optical measurements were performed with an electro-optic setup based on a polarizing optical microscope (Olympus BH2) with hotstage (Linkam TMS94). By applying an ac field via a function generator (Keysight 33500B), the intensity of the transmitted light was detected by a photodiode (FLC electronics) in combination with an oscilloscope (Keysight 2004A). For sample preparation, we used single-side rubbed nylon liquid crystal test cells (AWAT Spółka zo.o, Poland) with a cell thickness of 1.6 μm, ITO electrode, and SiO_2 isolation layer between coating and electrode. The test cells were filled by capillary forces and reduced pressure at temperatures close above the clearing temperature into the isotropic phase. Finally, the sample was sealed with UV glue to avoid further solvent evaporation. Purification of formamide (Sigma Aldrich, 99.5%) was performed as follows: to prevent the solvent from ion contamination due to formamide hydrolysis, the water content was reduced by the use of a 3 Å molecular sieve (stirring at 50 °C for 3 h). After two successive vacuum distillations at reduced pressure (1–3) $\times 10^{-3}$ mbar (Bp. 44 °C), the solvent had a residual water content of 0.02 wt. % by Karl-Fischer titration (TitroLine *alpha plus*, SI Analytics) and a specific electric conductivity of 5–6 μS/cm (measured with laboratory conductometer *Cond 720*, InoLab).

APPENDIX B: IMPACT OF ION CONTENT

Solvent purity played an essential role for the electro-optical observation of the electroclinic effect. In order to check how

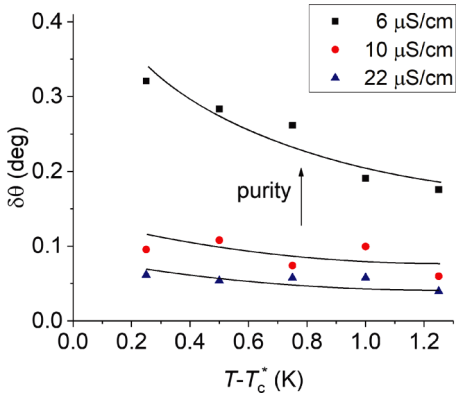

FIG. 11. Extrapolated values of the electroclinic tilt for three lyotropic L_α^* phases with constant solvent content of 18 wt. %, but increasing solvent purity. Measurements of the electroclinic tilt angle were carried out in an electric field of 2 V/μm at an electrode distance of 1.6 μm.

far the ion content influences the electroclinic response, we prepared samples with similar solvent content, but increasing ion content. We mixed purified formamide (see purification procedure above) with small amounts of nonpurified formamide (Sigma Aldrich, 99.5%) and obtained electrolyte solutions with increasing ion content. The values of the specific conductivity (measured before the addition of amphiphile) served as a qualitative measure of the increasing ion content of the lyotropic sample. The solvent purity had strong impact on the magnitudes of the measured electroclinic effect. Figure 11 shows the electroclinic director tilt of a lamellar L_α^* phase with 18 wt. % formamide close to the lyo-Sm-C^* transition. Already minor impurity (red and blue dots) had a significant impact on the amplitude of the electro-optic response. At a high ion content, the electroclinic effect came close to the detection limit of our electro-optical setup. This fact clearly points out the importance of the solvent purity, which strongly dominates the magnitude of the electroclinic response.

[1] S. Garoff and R. B. Meyer, Phys. Rev. A **19**, 338 (1979).
[2] S. Garoff and R. B. Meyer, Phys. Rev. Lett. **38**, 848 (1977).
[3] G. Andersson, I. Dahl, P. Keller, W. Kuczyński, S. Lagerwall, K. Skarp, and B. Stebler, Appl. Phys. Lett. **51**, 640 (1987).
[4] R. B. Meyer, L. Liebert, L. Strzelecki, and P. Keller, J. Phys. Lett. **36**, 69 (1975).
[5] G. Andersson, I. Dahl, W. Kuczynski, S. Lagerwall, K. Skarp, and B. Stebler, Ferroelectrics **84**, 285 (1988).
[6] C. Bahr and G. Heppke, Phys. Rev. A **37**, 3179 (1988).
[7] N. Kapernaum, D. M. Walba, E. Korblova, C. Zhu, C. Jones, Y. Shen, N. A. Clark, and F. Giesselmann, Chem. Phys. Chem. **10**, 890 (2009).
[8] S.-i. Nishiyama, Y. Ouchi, H. Takezoe, and A. Fukuda, Jpn. J. Appl. Phys. **26**, L1787 (1987).
[9] S. T. Lagerwall, in *Handbook of Liquid Crystals*, edited by J. W. Goodby, P. J. Collings, T. Kato, C. Tschierske, H. F. Gleeson, and P. Raynes (Wiley-VCH, Weinheim, 2014), Vol. 4, p. 134.
[10] P. G. de Gennes, C. R. Acad. Sci., Paris **B274**, 142 (1972).
[11] S. Pikin and V. Indenbom, Phys. Usp. **21**, 487 (1978).
[12] R. Blinc and B. Zěkš, Phys. Rev. A **18**, 740 (1978).
[13] S. T. Lagerwall, *Ferroelectric and Antiferroelectric Liquid Crystals* (John Wiley & Sons, New York, 2008), Chap. 5.9, pp. 147–154.
[14] S. T. Lagerwall, B. Otterholm, and K. Skarp, Mol. Cryst. Liq. Cryst. **152**, 503 (1987).
[15] F. Gouda, G. Andersson, S. Lagerwall, K. Skarp, B. Stebler, T. Carlsson, B. Žekš, C. Filipič, and A. Levstik, Liq. Cryst. **6**, 219 (1989).
[16] A. Jákli, J. Harden, C. Notz, and C. Bailey, Liq. Cryst. **35**, 395 (2008).
[17] J. Harden, N. Diorio, A. G. Petrov, and A. Jakli, Phys. Rev. E **79**, 011701 (2009).
[18] J. R. Bruckner, J. H. Porada, C. F. Dietrich, I. Dierking, and F. Giesselmann, Angew. Chem. Int. Ed. **52**, 8934 (2013).
[19] J. R. Bruckner, F. Knecht, and F. Giesselmann, Chem. Phys. Chem. **17**, 86 (2016).
[20] L. M. Blinov, S. A. Davidian, A. G. Petrov, A. T. Todorov, and S. V. Yablonskii, JETP Lett. **48**, 285 (1988).
[21] J.-H. Fuhrhop and W. Helfrich, Chem. Rev. **93**, 1565 (1993).
[22] G. Nounesis, B. R. Ratna, S. Shin, R. S. Flugel, S. N. Sprunt, A. Singh, J. D. Litster, R. Shashidhar, and S. Kumar, Phys. Rev. Lett. **76**, 3650 (1996).
[23] A. G. Petrov, *The Lyotropic State of Matter: Molecular Physics and Living Matter Physics*, Ferroelectricity of Lyotropics (Gordon and Breach Science Publishers, New York, 1999), Chap. 7, Sec. 7.9.
[24] Y. S. Negi, Y. Suzuki, T. Hagiwara, I. Kawamura, N. Yamamoto, K. Mori, Y. Yamada, M. Kakimoto, and Y. Imai, Liq. Cryst. **13**, 153 (1993).
[25] M. Skarabot, S. Kralj, R. Blinc, and I. Musevic, Liq. Cryst. **26**, 723 (1999).
[26] S. Seomun, V. P. Panov, and J. K. Vij, Ferroelectrics **278**, 151 (2002).
[27] T. P. Rieker, N. A. Clark, G. S. Smith, D. S. Parmar, E. B. Sirota, and C. R. Safinya, Phys. Rev. Lett. **59**, 2658 (1987).
[28] N. Hiji, A. D. L. Chandani, S.-I. Nishiyama, Y. Ouchi, H. Takezoe, and A. Fukuda, Ferroelectrics **85**, 99 (1988).
[29] N. A. Clark, T. P. Rieker, and J. E. Maclennan, Ferroelectrics **85**, 79 (1988).
[30] N. A. Clark and T. P. Rieker, Phys. Rev. A **37**, 1053 (1988).
[31] Y. Takanishi, Y. Ouchi, H. Takezoe, and A. Fukuda, Jpn. J. Appl. Phys. **28**, L487 (1989).
[32] J. R. Bruckner, D. Krueerke, J. H. Porada, S. Jagiella, D. Blunk, and F. Giesselmann, J. Mater. Chem. **22**, 18198 (2012).
[33] K. S. Cole and R. H. Cole, J. Chem. Phys. **9**, 341 (1941).
[34] B. Maximus, C. Colpaert, A. d. Meyere, H. Pauwels, and H. Plach, Liq. Cryst. **15**, 871 (1993).
[35] K. Neyts, S. Vermael, C. Desimpel, G. Stojmenovik, A. Verschueren, D. De Boer, D. de Boer, R. Snijkers, P. Machiels, and A. van Brandenburg, J. Appl. Phys. **94**, 3891 (2003).
[36] H. De Vleeschouwer, A. Verschueren, F. Bougrioua, K. Neyts, G. Stojmenovik, S. Vermael, and H. Pauwels, Jpn. J. Appl. Phys. **41**, 1489 (2002).

[37] H. De Vleeschouwer, A. Verschueren, F. Bougrioua, R. Van Asselt, E. Alexander, S. Vermael, K. Neyts, and H. Pauwels, Jpn. J. Appl. Phys. **40**, 3272 (2001).
[38] R. James, G. Stojmenovik, C. Desimpel, S. Vermael, F. A. Fernández, S. E. Day, and K. Neyts, J. Disp. Technol. **2**, 237 (2006).
[39] K. H. Yang, T. C. Chieu, and S. Osofsky, Appl. Phys. Lett. **55**, 125 (1989).
[40] M. Guena, Z. Y. Wu, and R. Vanderhagen, Ferroelectrics **188**, 201 (1996).
[41] E. D. Ley, V. Ferrara, C. Colpaert, B. Maximus, A. D. Meyere, and F. Bernardini, Ferroelectrics **178**, 1 (1996).
[42] Z. Zou, N. A. Clark, and M. A. Handschy, Ferroelectrics **121**, 147 (1991).
[43] K. Neyts and F. Beunis, Ferroelectrics **344**, 255 (2006).
[44] C. Colpaert, B. Maximus, and A. D. Meyere, Liq. Cryst. **21**, 133 (1996).
[45] J. M. Notley and M. Spiro, J. Chem. Soc. B **1996**, 362 (1966).
[46] L. Gorb, A. Asensio, I. Tuñón, and M. F. Ruiz-López, Chem. Eur. J. **11**, 6743 (2005).
[47] J. Thomas and D. F. Evans, J. Phys. Chem. **74**, 3812 (1970).
[48] T. Carlsson and I. Dahl, Mol. Cryst. Liq. Cryst. **95**, 373 (1983).
[49] F. Giesselmann and P. Zugenmaier, Phys. Rev. E **52**, 1762 (1995).
[50] F. Giesselmann, A. Heimann, and P. Zugenmaier, Ferroelectrics **200**, 237 (1997).
[51] F. Giesselmann, P. Zugenmaier, I. Dierking, S. T. Lagerwall, B. Stebler, M. Kašpar, V. Hamplová, and M. Glogarová, Phys. Rev. E **60**, 598 (1999).
[52] J. Hemine, A. Daoudi, C. Legrand, A. E. Kaaouachi, A. Nafidi, and H. Nguyen, Liq. Cryst. **37**, 1313 (2010).
[53] H. P. Padmini, N. V. Madhusudana, and B. Shivkumar, Bull. Mater. Sci. **17**, 1119 (1994).
[54] J. S. Kang, D. A. Dunmur, C. J. Booth, J. W. Goodby, and K. J. Toyne, Liq. Cryst. **20**, 109 (1996).
[55] J. Pavel and M. Glogarovaá, Ferroelectrics **114**, 131 (1991).
[56] J. R. Bruckner, *A First Example of a Lyotropic Smectic C* Analog Phase: Design, Properties and Chirality Effects* (Springer, New York, 2015).
[57] J. R. Bruckner, Ph.D. thesis, Universität Stuttgart, 2015.
[58] A. A. Kahwaji, O. Greffier, A. Leon, J. Rouch, and H. Kellay, Phys. Rev. E **63**, 041502 (2001).
[59] H.-P. Duwe, H. Engelhardt, A. Zilker, and E. Sackmann, Mol. Cryst. Liq. Cryst. **152**, 1 (1987).
[60] C. Y. Zhang, S. Sprunt, and J. D. Litster, Phys. Rev. E **48**, 2850 (1993).
[61] W. Helfrich, Z. Naturforsch., C **28**, 693 (1973).
[62] M. Hamm and M. Kozlov, Eur. Phys. J. E **3**, 323 (2000).